



ZnO nanoparticles attenuate polymer-wear-particle induced inflammatory osteolysis by regulating the MEK-ERK-COX-2 axis

Xiangchao Meng¹, Wei Zhang¹, Zhuocheng Lyu, Teng Long^{**}, You Wang^{*}

Department of Bone and Joint Surgery, Renji Hospital, School of Medicine, Shanghai Jiaotong University, 145 Middle Shandong Road, 200001, Shanghai, China

ARTICLE INFO

Keywords:

Inflammatory osteolysis
Mitogen-activated protein kinase pathway
Wear particle
Zinc oxide nanoparticles

ABSTRACT

Background/Objectives: Advanced thermoplastic materials, such as polyether-ether-ketone (PEEK) and highly cross-linked polyethylene (HXLPE), have been increasingly used as orthopaedic implant materials. Similar to other implants, PEEK-on-HXLPE prostheses produce debris from polymer wear that may activate the immune response, which can cause osteolysis, and ultimately implant failure. In this study, we examined whether the anti-inflammatory properties of zinc oxide nanoparticles (ZnO NPs) could attenuate polymer wear particle-induced inflammation.

Methods: RAW264.7 cells were cultured with PEEK or PE particles and gradient concentrations of ZnO NPs. Intracellular mRNA expression and protein levels of pro-inflammatory factors TNF- α , IL-1 β , and IL-6 were detected. An air pouch mouse model was constructed to examine the inflammatory response and expression of pro-inflammatory factors *in vivo*. Furthermore, an osteolysis rat model was used to evaluate the activation of osteoclasts and destruction of bone tissue induced by polymer particles with or without ZnO NPs. Protein expression of the MEK-ERK-COX-2 pathway was also examined by western blotting to elucidate the mechanism underlying particle-induced anti-inflammatory effects.

Results: ZnO NPs (≤ 50 nm, 5 $\mu\text{g}/\text{mL}$) showed no obvious cytotoxicity and attenuated PEEK or PE particle-induced inflammation and inflammatory osteolysis by reducing MEK and ERK phosphorylation and decreasing COX-2 expression.

Conclusion: ZnO NPs (≤ 50 nm, 5 $\mu\text{g}/\text{mL}$) attenuated polymer wear particle-induced inflammation via regulation of the MEK-ERK-COX-2 axis. Further, ZnO NPs reduced bone tissue damage caused by particle-induced inflammatory osteolysis.

The translational potential of this article: Polymer wear particles can induce inflammation and osteolysis in the body after arthroplasty. ZnO NPs attenuated polymer particle-induced inflammation and inflammatory osteolysis. Topical use of ZnO NPs and blended ZnO NP/polymer composites may provide promising approaches for inhibiting polymer wear particle-induced inflammatory osteolysis, thus expanding the range of polymers used in joint prostheses.

1. Introduction

Polyether-ether-ketone (PEEK) is an innovative alternative to conventional metallic material used in joint prostheses [1–3]. Conventional metal implant can produce stress in concentrated areas due to high elastic modulus and generate wear debris which induces peri-prosthetic osteolysis and implant loosening [4–6]. In contrast, PEEK has a modulus similar to that of bone, which greatly reduces stress shielding, and the risk of periprosthetic bone resorption [1,2,7,8]. PEEK is also

radiolucent and compatible with magnetic resonance imaging, which facilitates postoperative follow-up inspection and early detection of osteolysis [9]. The newly developed PEEK-on-highly cross-linked polyethylene (HXLPE) prosthesis has demonstrated biological safety and applicability in animals [2,10]. Unlike metal-on-metal or metal-on-HXLPE joint prostheses, PEEK-on-HXLPE prosthesis shows a modulus similar to that of cortical bone, which can improve patient comfort and extend implant lifetime by reducing the stress-shielding effect [1,6,11]. However, use of the PEEK-on-HXLPE prosthesis is

* Corresponding author.

** Corresponding author.

E-mail addresses: longteng@renji.com (T. Long), drwangyou@126.com (Y. Wang).

¹ These authors contributed equally.

limited by the production of PEEK and PE wear particles, which could activate macrophages and stimulate cells to express pro-inflammatory chemokines, such as interleukin (IL)-1 β , IL-6, IL-17, and tumour necrosis factor- α (TNF- α) [10,12,13]. These inflammatory factors can promote the formation and activation of osteoclasts and inhibit osteoblast formation, eventually leading to osteolysis and prosthesis loosening [14–17].

Many researches have been conducted to reduce wear particle-induced aseptic loosening of total joint replacements (TJRs). For example, composite materials containing zinc oxide nanoparticles (ZnO NPs) and FHBP-functionalised titanium have been found to suppress the inflammatory response and enhance the bone regeneration [18,19]. Polymer composites incorporating ZnO NPs could improve tribological performance and consequently decrease the production of wear debris [20]. In addition, ZnO NPs possess anti-inflammatory properties and exert protective effects on chondrocytes in the hypoxic environment [21, 22]. However, the anti-inflammatory and chondroprotective properties of ZnO NPs may depend on their size, shape, concentration, and experimental conditions [21–23]. Thus, the effect of ZnO NPs on inflammation induced by PEEK or PE wear debris requires further investigation.

Previous studies have shown that ZnO NPs influence the phagocytosis and autophagy of macrophages and suppress the activation of macrophages stimulated with lipopolysaccharide (LPS) [21,24,25]. We hypothesised that ZnO NPs have anti-inflammatory properties that could attenuate the inflammatory response induced by PEEK and PE polymer particles. Our research goal was to assess whether increasing the wear resistance and lubricating properties of these polymer materials and attenuating the inflammatory response induced by wear particles might be achieved by blending polymer particles with ZnO NPs. The aim of the present study was to investigate the effects of ZnO NPs on polymer particle-induced inflammation and the underlying mechanism.

2. Materials and methods

2.1. Material characterisation

The surface morphologies of ZnO NPs (quantum dot scale: ≤ 5 nm [Shanghai Bojiao Biotech Co., Shanghai, China]; nanoscale: ≤ 50 nm [Sigma-Aldrich, St. Louis, MO, USA], and microscale: ≤ 1 μ m [Sigma-Aldrich]), PEEK particles (Zeniva PEEK ZA-500), and PE particles (Chirulen HXLPE 1020X) were characterised using a Hitachi SU8010 field-emission scanning electron microscope (SEM; Hitachi, Tokyo, Japan) and/or a Tecnai-12 transmission electron microscope (TEM; Philip Apparatus Co., Amsterdam, The Netherlands). SEM images and TEM spectra were obtained at 2 and 200 kV acceleration, respectively. All measurements were performed in triplicate. Prior to use, PEEK and PE particles were ultrasonicated in ethanol, vacuum-dried to remove the solvent, and subsequently sterilised with ethylene oxide after ball milling. The average sizes of the PEEK and PE wear particles were comparable: PE particle size diameter ranged from 0.22 to 31.11 μ m with an average diameter of 1.66 μ m, while PEEK particle size diameter ranged from 0.25 to 46.47 μ m with an average diameter of 1.05 μ m [2,10,13].

2.2. Cell culture

RAW264.7 cells were obtained from the Cell Bank at the Chinese Academy of Science (Shanghai, China). Cells were maintained in α -minimum essential medium (HyClone™ Laboratories, Logan, UT, USA) with 10% foetal bovine serum (Gibco, Grand Island, NY, USA) and 1% penicillin/streptomycin at 37 °C in a 5% CO₂ incubator. The growth medium was refreshed every 2 days.

RAW264.7 cells were seeded into a 96-well plate at 1×10^3 cells/well. Different sizes (quantum dot scale: ≤ 5 nm; nanoscale: ≤ 50 nm; and microscale: ≤ 1 μ m) and concentrations (0, 5, 10, 15, and 20 μ g/mL) of ZnO NPs were co-cultured with cells for 24 h. Cell cytotoxicity was detected using the CCK-8 assay. RAW 264.7 cells were seeded into a 6-

Table 1

Primer sequences of mouse inflammatory genes used in RT-PCT.

Target Gene	Forward Primer Sequence (5'-3')	Reverse Primer Sequence (5'-3')
<i>β-Actin</i>	CTACCTCATGAAGATCCTGACC	CACAGCTTCTCTTTGATGTCAC
<i>IL-1β</i>	TCGCAGCAGCACATCAACAAGAG	TGCTCATGTCCTCATCCTGGAAGG
<i>IL-6</i>	CTGCAAGAGACTTCCATCCAG	GACCTTGAGGTTGACCTTCACAT
<i>Tnf-α</i>	ATGTCTCAGCCTTCTCTCATTC	GCTTGTCACCTGAATTTTGAGA

well plate at 1×10^6 cells/well. ZnO NPs of different sizes (1 μ g/mL) and PE particles (10⁸) were cocultured with cells in four groups: PE; PE + ZnO (≤ 5 nm); PE + ZnO (≤ 50 nm); PE + ZnO (≤ 1 μ m). The supernatant was collected after 24 h to measure pro-inflammatory factor expression using enzyme-linked immunosorbent assay (ELISA).

PEEK (10⁸) and PE (10⁸) particles and ZnO NPs (≤ 50 nm; 1, 5, and 10 μ g/mL) were added to different wells at a particle-to-cell ratio of 100:1. The supernatant was collected after incubation for 6 h and 24 h to measure levels of pro-inflammatory factors using ELISA. Total RNA and protein were also extracted and analysed using real-time PCR and western blotting.

2.3. ELISA

Levels of pro-inflammatory factors IL-1 β , IL-6, and TNF- α in the cell medium supernatant were measured using an ELISA kit (MultiSciences (Lianke) Biotech Co., Ltd., Hangzhou, China), according to the manufacturer's protocols.

2.4. Real-time PCR

Total RNA was extracted using TRIzol™ reagent (Invitrogen, Carlsbad, CA, USA) and total RNA extraction kit (QIAGEN, Hilden, Germany). Approximately 1 μ g RNA was reverse-transcribed into cDNA using the PrimeScript™ reverse transcription kit (TaKaRa Bio, Shiga, Japan) according to the manufacturer's protocol. Expression levels of *IL-1 β* , *IL-6*, *Tnf- α* , and *β -Actin* were examined using an ABI 7500 real-time PCR system (Applied Biosystems, Foster City, CA, USA). *β -Actin* was used as a reference gene to normalise gene expression. The results were expressed using the 2^{- $\Delta\Delta$ CT} method. The primer sequences used in real-time PCR analysis are listed in Table 1 [26].

2.5. Western blot analysis

Proteins were extracted using 1 \times RIPA lysis buffer (Thermo Fisher Scientific, Waltham, MA, USA) containing a phosphatase and protease inhibitor cocktail (Thermo Fisher Scientific). Western blotting was performed following standard procedures. Briefly, protein lysates were separated using 10% sodium dodecyl sulphate-polyacrylamide gel electrophoresis and then transferred onto polyvinylidene fluoride membranes (PVDF; Thermo Fisher Scientific). After blocking with blocking reagent (Thermo Fisher Scientific), the membranes were incubated overnight with primary antibodies at 4 °C. After incubation with secondary antibodies, the PVDF membranes were thoroughly washed and detected using electrochemiluminescence solution (Thermo Fisher Scientific). Primary antibodies (MEK1/2, P-MEK1/2, ERK1/2, P-ERK1/2, COX-2, P65, P-P65, I κ B α , P-I κ B α , and GAPDH) and secondary antibodies were purchased from Cell Signaling Technology (Danvers, MA, USA) [26].

2.6. Air pouch mouse model

An air pouch mouse model was used to assess the effects of different particles. Forty-two nude mice (BALB/c) were purchased from the Shanghai Institute of Zoology (Chinese Academy of Sciences). The animal studies were performed in accordance with the Animal Care and Use

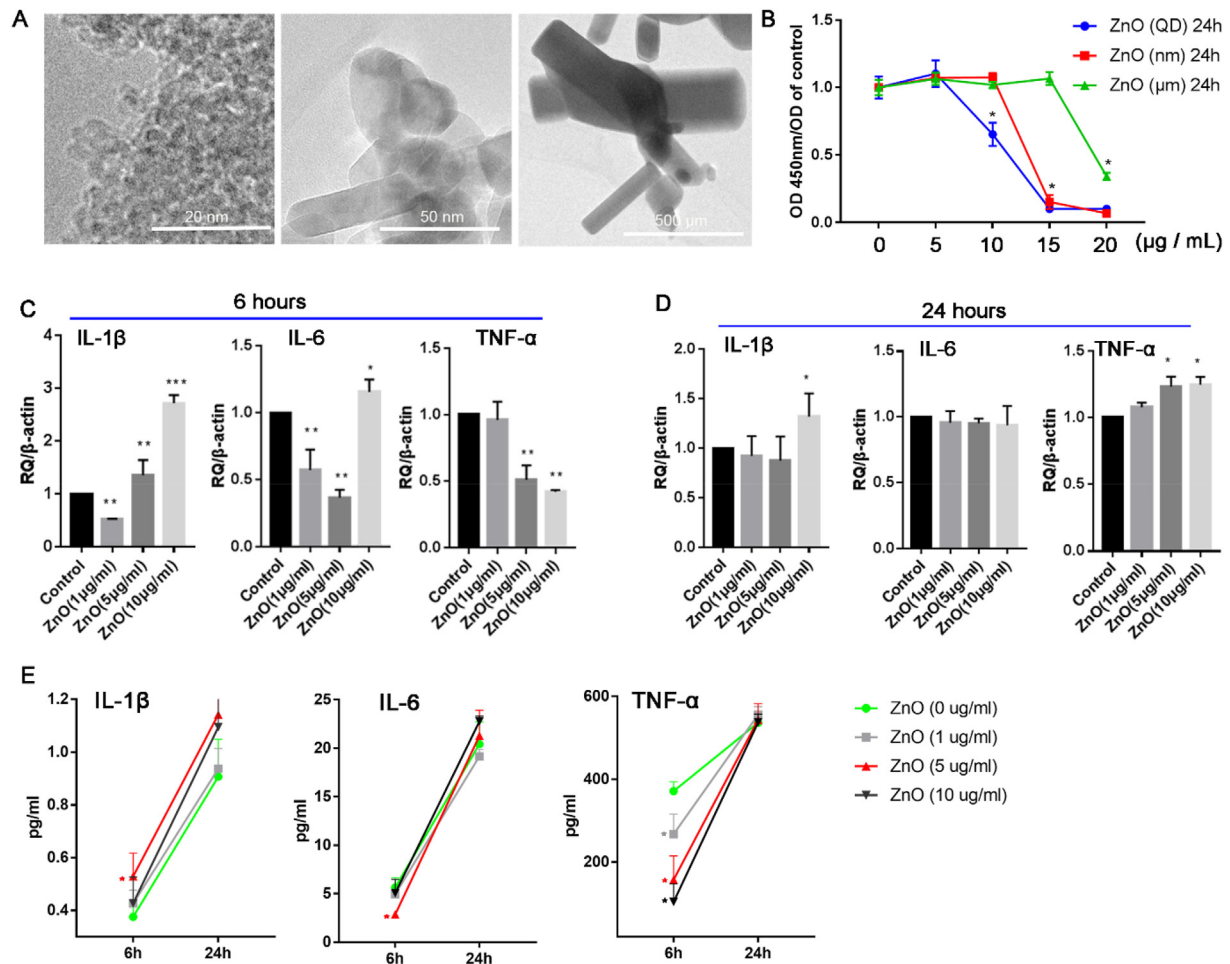


Figure 1. Zinc oxide nanoparticles (ZnO NPs) are not cytotoxic and do not induce a significant cellular inflammatory response at low concentration *in vitro*. The morphology (A) and cytotoxicity (B) of different sized ZnO NPs. mRNA expression of *IL-1β*, *IL-6*, and *Tnf-α* in cells co-cultured with ZnO NPs (1, 5, and 10 µg/mL) for 6 h and 24 h (C and D). Protein expression of IL-1β, IL-6, and TNF-α in the supernatant after co-culturing cells with different concentrations of ZnO NPs (1, 5, and 10 µg/mL) for 6 h and 24 h (E). **p* < 0.05; ***p* < 0.01.

Committee Guidelines of the Shanghai Jiao Tong University School of Medicine. The animals were divided into six groups: control (normal saline, NS), ZnO, PEEK, PEEK + ZnO, PE, and PE + ZnO. First, 5 mL gas was injected subcutaneously into the back of each mouse to create an air pouch. Thereafter, gas was reinjected every 2 days to maintain the air pouch. After three weeks, when the air pouch had stabilised, 1 mL solution containing pure saline, ZnO NPs (5 µg/mL), PEEK (10¹¹ particles), PEEK (10¹¹ particles) + ZnO NPs (5 µg/mL), PE (10¹¹ particles), or PE (10¹¹ particles) + ZnO NPs (5 µg/mL) was injected into the mouse air pouch. After 2 weeks, the animals were sacrificed by cervical dislocation, the air pouches were collected, and specimens were embedded in paraffin [27].

2.7. Haematoxylin & eosin and immunohistochemical staining

The paraffin-embedded specimens were sliced into 5 µm-thick sections using a microtome, deparaffinised via three changes of xylene, and then rehydrated using a gradient of ethanol and distilled water. Haematoxylin & eosin (H&E) staining was performed using a standard protocol, and sections were dehydrated using a reverse gradient of ethanol and xylene [26].

Immunohistochemical staining was performed as follows. Briefly, antigen retrieval was performed with sodium citrate solution (pH 6.5) at 65 °C for 30 min. After re-equilibrating to room temperature, the sections were rinsed three times with phosphate-buffered saline (PBS). The

sections were then incubated with 3% hydrogen peroxide for 10 min and washed with PBS. Blocking was performed using 3% horse serum for 30 min. Incubation with the primary antibodies was performed overnight at 4 °C. On the following day, the sections were washed with PBS and incubated with the secondary antibodies for 1 h at room temperature. After extensive washing with PBS, colour-developing and counter-staining were performed using a Vectastain ABC kit (Vector Laboratories, Burlingame, CA, USA) with haematoxylin [13].

2.8. Cell mean density

The brown granules staining was considered positive. Image-Pro Plus version 6.0 software (Medical Cybernetics, Inc., Rockville) was used to assess the cell number and the integrated optical density (IOD) value of the of the positive region. The cell mean densitometry of the digital image was obtained by calculating IOD/positive cell number, and was designated as representative IL-1β, IL-6, and TNF-α staining intensity (indicating the relative expression level).

2.9. In vivo evaluation of osteolysis

2.9.1. Rat osteolysis model

Twenty-four Sprague–Dawley rats (3-months-old, female) were obtained from the Shanghai Institute of Zoology (Chinese Academy of Sciences). The animal studies were performed in accordance with

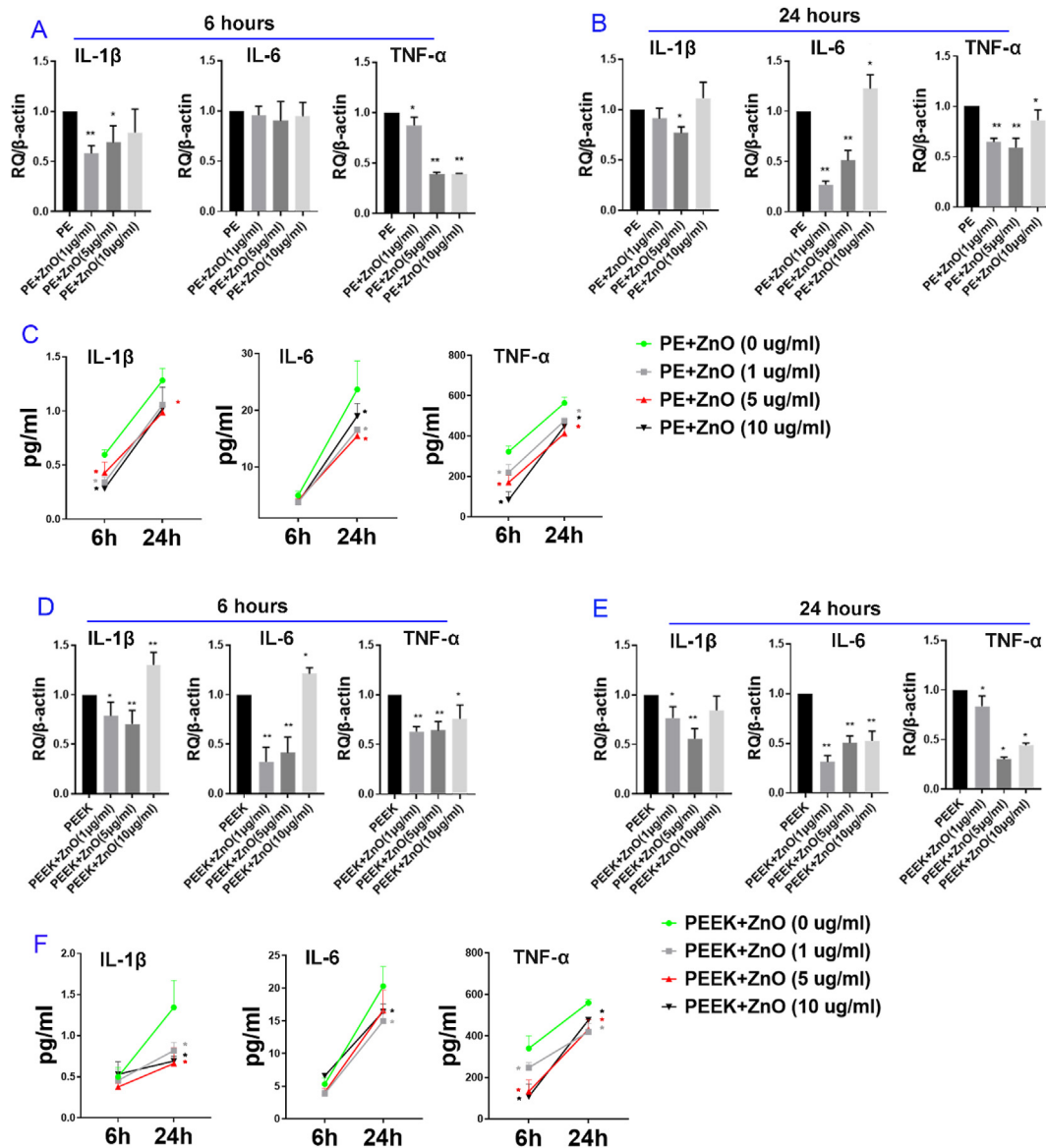


Figure 2. Zinc oxide nanoparticle (ZnO NPs) attenuate polymer-particle-induced inflammation *in vitro*. mRNA expression of *Il-1β*, *Il-6*, and *Tnf-α* in RAW264.7 cells after co-culturing cells with different concentrations of ZnO NPs (1, 5, and 10 $\mu\text{g}/\text{mL}$) and polyethylene (PE) particles for 6 h and 24 h (A and B). Protein expression of IL-1 β , IL-6, and TNF- α in the supernatant of RAW264.7 cells co-cultured with different concentrations of ZnO NPs and PE particles for 6 h and 24 h (C). mRNA expression of *Il-1β*, *Il-6*, and *Tnf-α* in cells after being co-cultured with different concentrations of ZnO NPs (1, 5, and 10 $\mu\text{g}/\text{mL}$) and polyether-ether-ketone (PEEK) particles for 6 h and 24 h (D and E). Protein expression of IL-1 β , IL-6, and TNF- α in the supernatant of RAW264.7 cells co-cultured with different concentrations of ZnO NPs and PEEK particles for 6 h and 24 h (F). * $p < 0.05$; ** $p < 0.01$.

Shanghai Jiao Tong University School of Medicine Animal Care and Use Committee Guidelines. After being anaesthetised with chloral hydrate, the animals were disinfected with iodophor. The left knee joint was exposed, a syringe needle was placed into the femoral medullary cavity, and either 0.5 mL solution of PEEK or PE particles or a mixture of polymer particles plus ZnO NPs (5 $\mu\text{g}/\text{mL}$) was injected into the bone marrow. After four weeks, the rats were sacrificed by cervical dislocation, and the femoral segment of the left hindlimb was obtained [28].

2.9.2. Microcomputed tomography (micro-CT) and section staining

Damaged bone around the particles was detected using the GE Explore Locus SP Micro-CT (GE Healthcare, Chicago, IL, USA), and 3D images were reconstructed. The bone volume fraction (bone volume/total volume) and trabecular pattern factor were determined using Sky-Scan DataViewer and CTAn software (Bruker, Karlsruhe, Germany). The region of interest was from the growth plate to the trabecular bone under

the growth plate with a thickness of 200 micro-CT layers [2].

2.9.3. H&E and TRAP staining

After fixation in 4% paraformaldehyde, samples were decalcified using EDTA, and dehydrated using a 75–100% alcohol gradient. Samples were embedded in paraffin, and sliced into 5 μm sections. H&E and tartrate-resistant acid phosphatase (TRAP) staining was performed using standard protocols [29].

2.9.4. Statistical analysis

All data are expressed as the mean \pm SD obtained from triplicate independent experiments. One-way analysis of variance (ANOVA) and Tukey's multiple comparison test were used to evaluate statistically significant differences among groups. All statistical analyses were performed using GraphPad Prism 7.0 statistical software (GraphPad, Inc., La Jolla, CA, USA). A p -value < 0.05 was considered statistically significant.

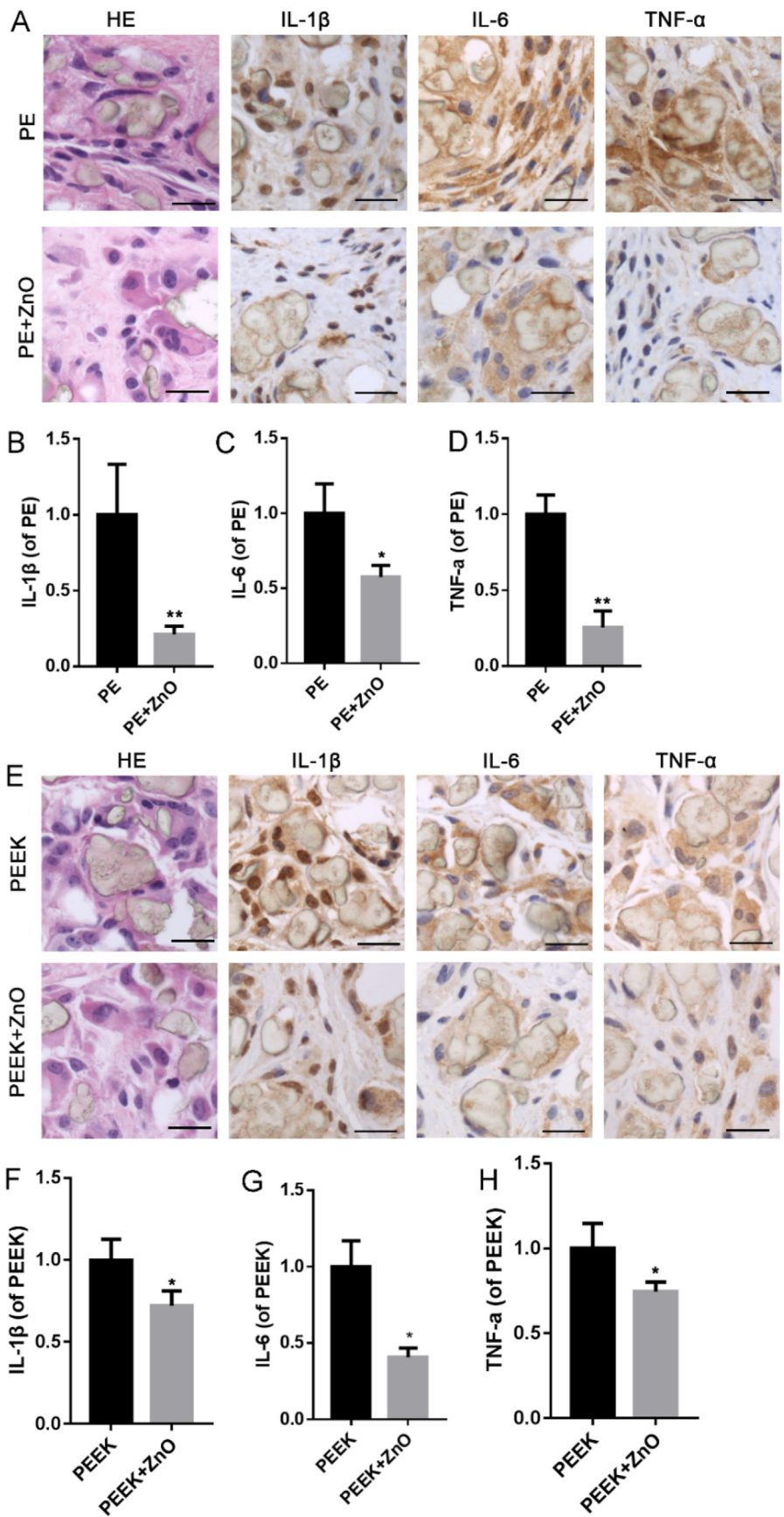


Figure 3. Zinc oxide nanoparticles (ZnO NPs) attenuate polymer particle-induced inflammation in the air pouch mouse model. Immunohistochemical staining (A) and analysis of IL-1 β (B), IL-6 (C), and TNF- α (D) expression after stimulation with polyethylene (PE) particles and ZnO NPs + PE particles. Immunohistochemical staining (E) and analysis of IL-1 β (F), IL-6 (G), and TNF- α (H) expression after stimulation with polyether-ether-ketone (PEEK) particles and PEEK particles + ZnO NPs. Positive staining, displayed as fine dark brown granules, is mainly confined to the cytoplasm. Black scale bars = 10 μm * p < 0.05; ** p < 0.01.

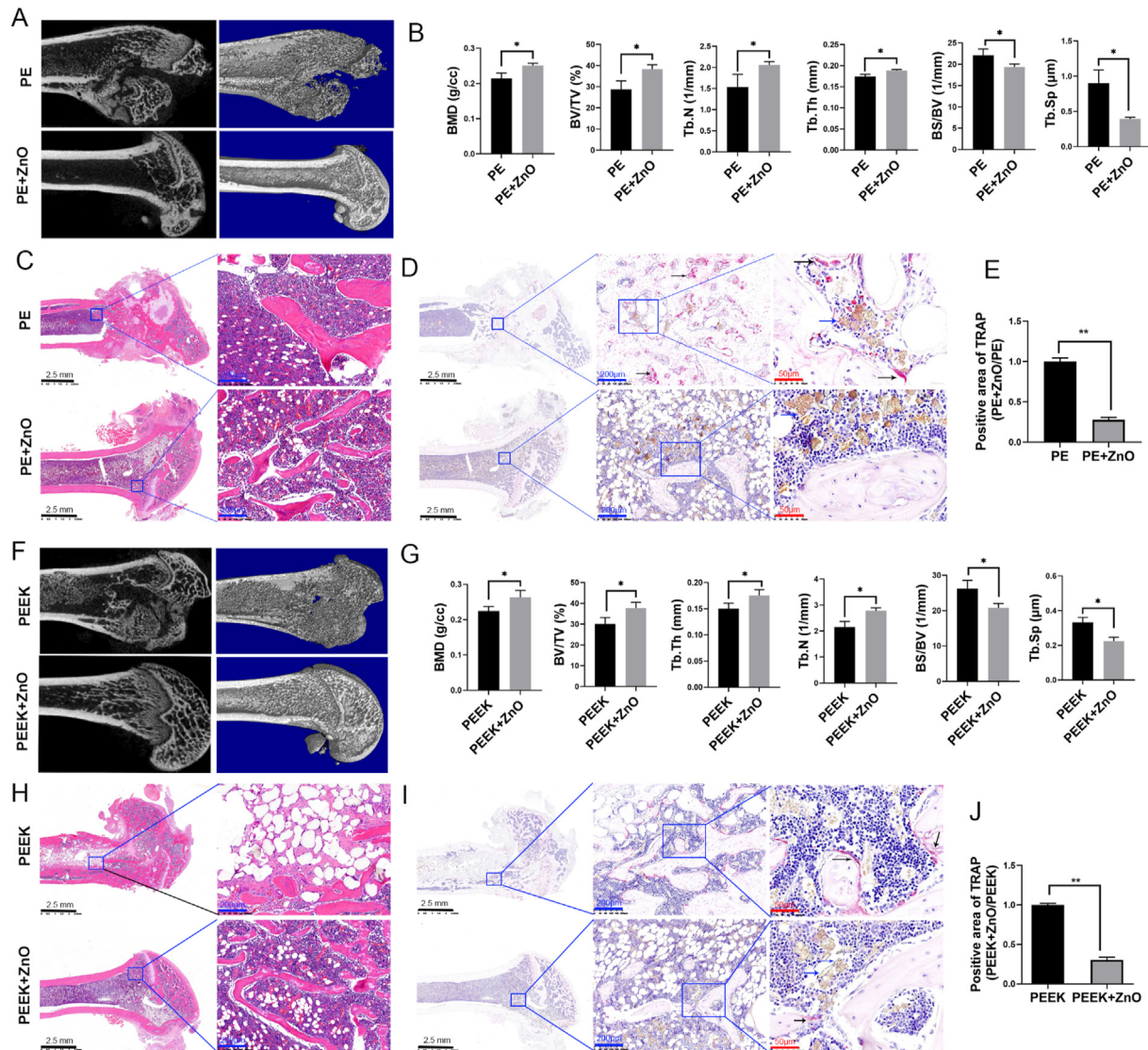


Figure 4. Zinc oxide nanoparticles (ZnO NPs) attenuate polymer particle-induced inflammatory osteolysis in a rat model. Micro-CT images and histological analysis of the polyethylene (PE) and zinc oxide nanoparticle (ZnO NP) + PE groups (**A and B**). Haematoxylin and eosin (H&E) staining (**C**) and TRAP staining (**D and E**) of the PE and ZnO + PE groups. Micro-CT images and histological analysis of the polyether-ether-ketone (PEEK) and ZnO NP + PEEK groups (**F and G**). H&E staining (**H**) and TRAP staining (**I and J**) of the PEEK and ZnO NP + PEEK groups. The cytoplasm of activated osteoclasts appears dark red in TRAP staining. The black arrow indicates activated osteoclasts, the blue arrow indicates polymer particles. Black scale bars = 2.5 mm; blue scale bars = 200 µm; red scale bars = 50 µm **p* < 0.05; ***p* < 0.01.

3. Results and discussion

3.1. ZnO NPs are not cytotoxic and do not induce a significant cellular inflammatory response at low concentration *in vitro*

Previous studies have suggested that ZnO NPs (<10 µg/mL) could attenuate the phagocytic function and activation of macrophages and that their cytotoxicity is related to particle size [23–25]. The results of the present study indicated that ZnO NPs were not cytotoxic at low concentrations (≤5 µg/mL), but their cytotoxicity significantly increased with increasing concentration (>10 µg/mL) (Fig. 1A). In addition, ZnO NP cytotoxicity was related to particle size, with smaller particles exerting greater cytotoxic effects than larger particles at the same concentrations (Fig. 1B). In agreement with previous findings, these results suggest that smaller NPs have larger surface areas and more exposed reactive sites, which lead to higher toxicity and more oxygen free radicals [23,30–32]. Furthermore, co-culturing cell with different sizes of ZnO NPs (1 µg/mL) and PE particles (10⁸) (Fig. S1A) indicated that only nanoscale ZnO particles (≤50 nm) significantly reduced the expression of

IL-1β, IL-6, IL-12, and TNF-α in the cell supernatant induced by PE particles (Fig. S1B). Meanwhile, co-culturing cells with ZnO NPs of different concentrations (1, 5, and 10 µg/mL) revealed that mRNA expression levels of *Il-1β*, *Il-6*, and *Tnf-α* in the cell supernatant were significantly decreased in the 5 µg/mL group at 6 h and negligibly different from those in the control group at 24 h (Fig. 1C and D). Additionally, protein expression levels of IL-6 and TNF-α in the cell supernatant were significantly decreased in the 5 µg/mL group at 6 h and negligibly different from those in the control group at 24 h (Fig. 1E). These results indicated that nanoscale ZnO NPs (≤50 nm) at low concentration (5 µg/mL) were biosafe and had an anti-inflammatory effect *in vitro* (Figs. 1 and S1).

3.2. ZnO NPs attenuate polymer-particle-induced inflammation *in vitro*

Wear debris from PEEK-on-HXLPE includes PEEK and ultra-high-molecular-weight PE (UHMWPE) particles [10]. Although wear debris ranges in size from tens of nanometres to hundreds of microns, debris with a diameter of 0.1–10 µm is the most biologically active [33]. In particular, debris approximately 1 µm in diameter is easily engulfed by

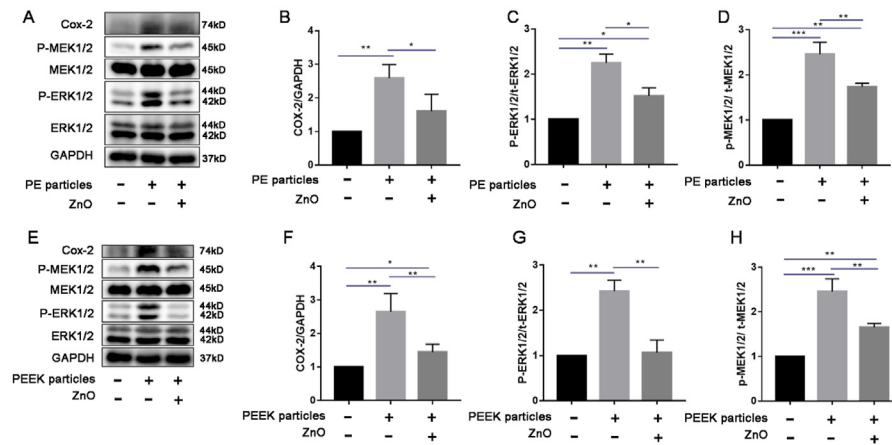


Figure 5. Zinc oxide nanoparticles (ZnO NPs) regulate p-MEK/p-ERK and COX-2 expression induced by polymer particles *in vitro*. Western blot images and analysis of COX-2 (A and B), t-ERK1/2 (A), p-ERK1/2 (A and C), t-MEK1/2 (A), and p-MEK1/2 (A and D) expression in the control, polyethylene (PE), and PE + ZnO NP groups. Western blot images and analysis of COX-2 (E and F), t-ERK1/2 (E), p-ERK1/2 (E and G), t-MEK1/2 (E), and p-MEK1/2 (E and H) expression in the control, polyether-ether-ketone (PEEK), and PEEK + ZnO NP groups. * $p < 0.05$; ** $p < 0.01$.

macrophages and induces inflammatory responses [33–35]. Previous research reported that wear debris from PEEK-on-HXLPE prostheses was close to 1.25 μm in diameter [10], which is similar to that of the polymer particles in the present study (Fig. S1A). Given aforementioned results, nanoscale ZnO NPs at size ≤ 50 nm were used to determine the optimal concentration for attenuating cellular inflammatory responses induced by PE and PEEK particles. Cells were cultured ZnO NPs (≤ 50 nm) at different concentrations (0, 1, 5, and 10 $\mu\text{g}/\text{mL}$) and PE particles (10^8). At 5 $\mu\text{g}/\text{mL}$, ZnO NPs (≤ 50 nm) significantly decreased the mRNA and protein expression of IL-1 β and TNF- α at 6 h and 24 h (Fig. 2A–C) in the absence of PEEK or PE particles. Although IL-6 mRNA and protein expression levels remained unaltered at 6 h, it was significantly decreased in the 5 $\mu\text{g}/\text{mL}$ group at 24 h (Fig. 2A–C). In the presence of PEEK particles (10^8), ZnO NPs (≤ 50 nm) at 5 $\mu\text{g}/\text{mL}$ significantly decreased mRNA expression levels of IL-1 β , IL-6, and TNF- α at 6 h and 24 h (Fig. 2D and E). The protein expression of IL-1 β and IL-6 at 6 h were negligibly different from those in the control group, but protein expression levels of IL-1 β , IL-6, and TNF- α were significantly decreased in the 5 $\mu\text{g}/\text{mL}$ group at 24 h (Fig. 2F). Although the results in Fig. 2 suggested that the expression of pro-inflammatory cytokines was decreased in the 1 and 10 $\mu\text{g}/\text{mL}$ groups, the attenuated effect on pro-inflammatory factors was greater in the 5 $\mu\text{g}/\text{mL}$ group. These results further supported that nanoscale ZnO NPs (≤ 50 nm) at low concentration (5 $\mu\text{g}/\text{mL}$) were safe and reduced the inflammatory effect induced by polymer particles *in vitro* (Figs. 1 and 2).

3.3. ZnO NPs (5 $\mu\text{g}/\text{mL}$) attenuate polymer particle-induced inflammation and inflammatory osteolysis *in vivo*

Subsequently, the air pouch mouse model was used to investigate the effect of ZnO NPs on polymer particle-induced inflammation *in vivo*. Compared to normal saline, ZnO NP (5 $\mu\text{g}/\text{mL}$; 1 mL) injection alone did not induce a significant change in protein expression levels of IL-1 β , IL-6, and TNF- α compared to those in the control group (normal saline) (Fig. S2A–D); whereas PE and PEEK injection significantly increased protein expression IL-1 β , IL-6, and TNF- α (Figs. 3 and S2). Addition of ZnO NP significantly reduced the protein expression of IL-1 β , IL-6, and TNF- α compared to PE alone (Fig. 3A–D). Similarly, the PEEK + ZnO group exhibited decreased IL-1 β , IL-6, and TNF- α protein levels compared to those in the PEEK group (Fig. 3E–H). These results indicated that ZnO NPs (5 $\mu\text{g}/\text{mL}$) did not induce a significant tissue inflammatory response and attenuated the inflammatory response induced by polymer particles *in vivo*.

The osteolysis rat model was used to further investigate the effects of ZnO NPs on polymer particle-induced osteolytic disease. The results of

micro-CT and histological analysis revealed that the structural integrity of the distal femur was visibly destroyed in the PE and PEEK groups. In addition to the structure of the distal femur remaining intact, the bone density, bone volume/total volume, and trabecular bone number and thickness were higher in the PE + ZnO and PEEK + ZnO groups than in the PE and PEEK groups (Fig. 4A–C, F–H). Furthermore, the coefficient of variation of the trabecular bone was reduced in the PE + ZnO and PEEK + ZnO groups (Fig. 4B, G), suggesting a milder degree of osteoporosis than in the PE and PEEK groups. Positive TRAP staining can show the number and activation state of osteoclasts, which reflects the degree of bone destruction. In the present study, TRAP staining revealed that the PE + ZnO and PEEK + ZnO groups displayed significantly fewer osteoclasts than the PE and PEEK groups (Fig. 4D, E, I, and J). These results indicated that the activation of osteoclasts and destruction of bone tissue induced by PE and PEEK particles were attenuated by ZnO NPs.

Osteolysis and implant loosening induced by wear debris involve a multitude of cell populations, including osteoblasts, osteoclasts, and synovial fibroblasts [15,24,36]. For PEEK-on-HXLPE implants, the wear debris-induced inflammatory response is mostly driven by macrophages, which can release an array of proinflammatory mediators [10,13,33]. However, the role of macrophage stimulation by polymer particles in the development of osteolysis remains unclear. Therefore, the anti-inflammatory properties of ZnO NPs were used to investigate the mechanism by which macrophages were stimulated by polymer particles.

3.4. ZnO NPs regulate p-MEK/p-ERK and COX-2 expression induced by polymer particles *in vitro* and *in vivo*

COX-2 is an inducible enzyme responsible for initiating the inflammatory response in immune cells. The major products of COX-2 are prostaglandins, which are further processed into prostaglandin E2 (PGE2) [37]. COX-2 plays a direct role in implant-related osteolysis, which was previously demonstrated by COX-2 $^{-/-}$ mice exhibiting significantly reduced debris-induced osteolysis compared to wild-type mice [38]. However, the immunogenicity of wear particles is lower than that of biological stimuli because of their chemically inert properties [12,13,39], suggesting that the signalling pathways involved might be different. In the present study, the expression of key proteins in the NF- κ B and ERK pathways was evaluated to elucidate the mechanism underlying polymer particle stimulation of macrophages.

Protein expression levels of p-I κ B and p-P65 were increased in the PE and PEEK groups compared to those in the control group (Figs. S3A, B, E, and F) but were significantly decreased in the PE + ZnO and PEEK + ZnO groups compared to their respective polymer particle groups (Figs. S3C, D, G, and H). These results suggested that the NF- κ B pathway, which is

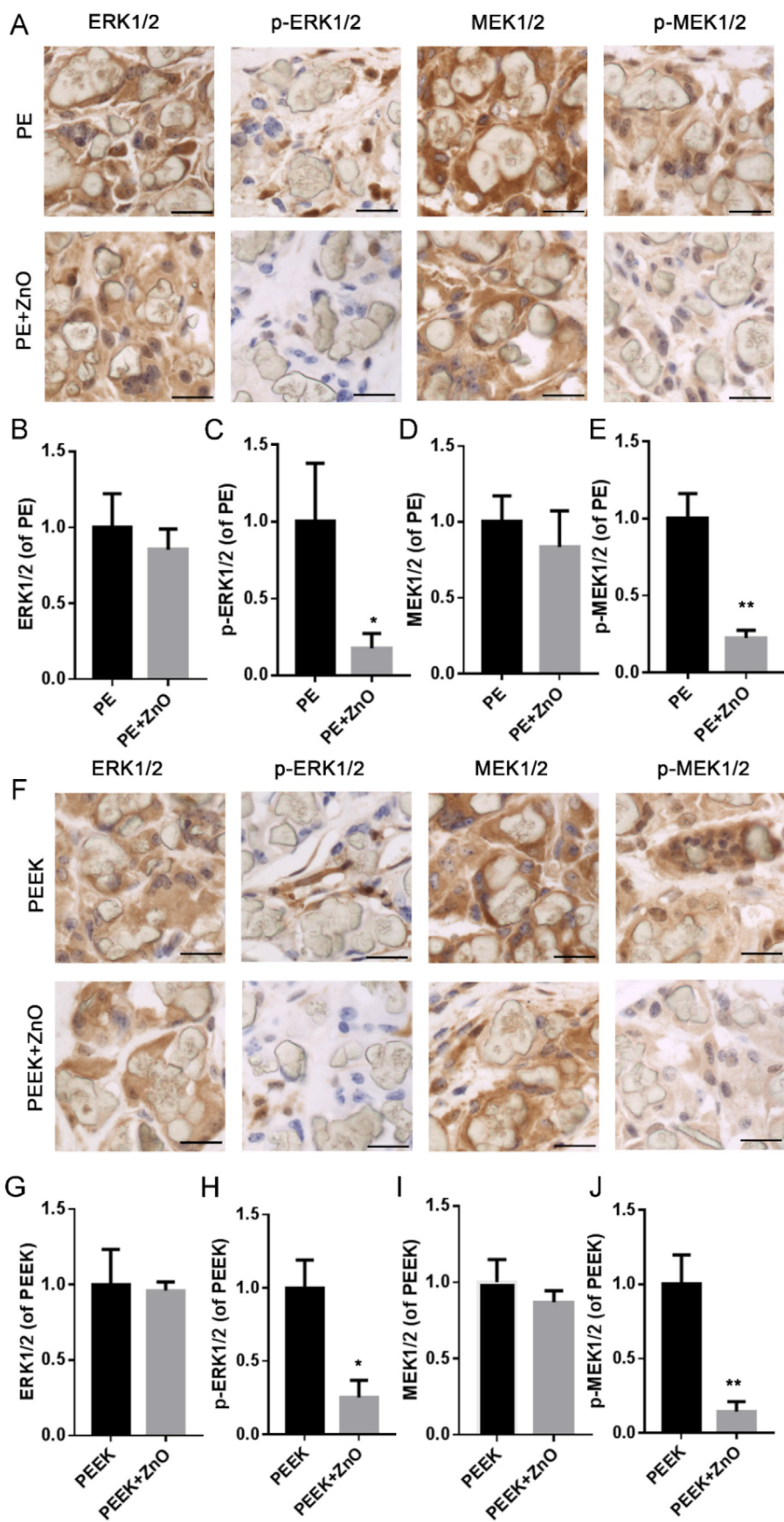


Figure 6. Zinc oxide nanoparticles (ZnO NPs) regulate p-MEK/p-ERK expression induced by polymer particles in the air pouch mouse model. Immunohistochemical staining and analysis of ERK1/2 (A and B), p-ERK1/2 (A and C), MEK1/2 (A and D), and p-MEK1/2 (A and E) expression the polyethylene (PE) and PE + ZnO NP groups. Immunohistochemical staining and analysis of ERK1/2 (F and G), p-ERK1/2 (F and H), MEK1/2 (F and I), and p-MEK1/2 (F and J) expression in the polyether-ether-ketone (PEEK) group and PEEK + ZnO NP groups. Black scale bars = 10 μm; **p* < 0.05; ***p* < 0.01.

rapidly activated in response to biological stimuli such as bacteria or LPS [36,38], was stimulated by the polymer particles. PDTC (pyrrolidine dithiocarbamate ammonium), a potent NF- κ B inhibitor that inhibits I κ B phosphorylation, prevents NF- κ B translocation into the nucleus and reduces the expression of downstream cytokines. Although protein expression levels of IL-1 β , IL-6, and TNF- α in the PE and PEEK groups were significantly increased compared to those in the control group (Fig. S4), proinflammatory cytokine levels remained higher than those in the control group after blocking the NF- κ B pathway with PDTC, particularly in the PE + PDTC group (Fig. S4). These results indicated that the NF- κ B pathway was only partially involved in the inflammatory response induced by polymer particles.

A recent study reported that inflammation induced by wear particles is closely related to the MAPK pathway, as blocking the ERK pathway could be used to treat or weaken the inflammatory response [40]. Indeed, the ERK and JNK pathways were activated as an early response to titanium (Ti) particles and participated in the WNT and BMP signalling pathways to suppress and subsequently inhibit osteogenesis [40]. Further, phagocytosis of Ti particles increased COX-2 and IL-6 production via ERK1/2–CEBP- β signalling [40].

In the current study, phosphorylation of ERK1/2 and MEK1/2 was significantly increased in the PE and PEEK groups *in vitro* compared to that in the control group (Fig. 5), whereas the expression of p-ERK1/2 and p-MEK1/2 decreased in the presence of ZnO NPs compared to that in the respective polymer particle groups (Fig. 5). Additionally, COX-2 protein levels were decreased in the ZnO NP-treated groups compared to those in the respective polymer particle groups but were higher than those in the control group (Fig. 5). Immunohistochemical staining revealed that the expression of t-ERK1/2 and t-MEK1/2 in the PE and PEEK groups did not differ significantly from that in the PE + ZnO and PEEK + ZnO groups (Fig. 6A, B, D, F, G, and I), but the expression of p-ERK1/2 and p-MEK1/2 was decreased in the PE + ZnO and PEEK + ZnO groups (Fig. 6A, C, E, F, H, and J). These results indicated that ZnO NPs may attenuate inflammatory osteolysis by inhibiting the MAPK/ERK kinase1/2 pathway.

COX-2 and its downstream product PGE2 have direct roles in promoting debris-induced implant-related osteolysis [38]. Wear debris reportedly induces an increase in PGE2 levels, which stimulates bone resorption via upregulation of RANKL and increases osteoclast activity [41]. Moreover, COX-2 inhibitors such as celecoxib and other nonsteroidal anti-inflammatory drugs have been shown to suppress wear debris-induced osteolysis in animal models [42]. Further, a previous study reported that COX-2 expression could be increased via activation of the ERK signalling pathway in bone marrow-derived murine macrophages [43]. Biometal has important roles in bone regeneration, including Ca, Mg, Zn, Cu, Mn, and Co. Zn and Mg are both essential mineral for the growth of bone. Zn and its alloys exhibit distinct advantages in promoting bone regeneration due to their capacity to stimulate osteoblast bone formation, increase alkaline phosphatase activity, and inhibit osteoclast differentiation [44]. Furthermore, Zinc, which is required for enzymes involved in DNA and RNA synthesis and is critical for maintaining cell functions, can stimulate zinc-sensing receptors and trigger downstream signalling involving the ERK/AKT pathway [43,45]. In the present study, ZnO NPs inhibited the MEK-ERK signalling pathway and reduced the production of COX-2, as well as that of pro-inflammatory cytokines. These results indicated that ZnO NPs attenuated the polymer particle-induced inflammatory response by downregulating COX-2 expression via the MEK-ERK pathway.

Macrophages are plastic cells that perform a wide spectrum of functions [46]. When exposed to external biological stimuli such as LPS and IFN- γ , macrophages are polarised to the M1-like phenotype, which produce pro-inflammatory cytokines [46]. When involved in tissue remodelling, macrophages are polarised to the M2-like phenotype and produce immune-suppressive cytokines such as TGF- β [46]. During aseptic loosening, inflammatory reactions are mainly driven by activated M1 macrophages, while M2 macrophages secrete immune-suppressive cytokines

to attenuate inflammation [18]. Previous studies have suggested that zinc modulates macrophage polarisation, and the critical roles of zinc in macrophage functions have been widely documented [18,21,25,30,45,47]. Thus, the results of the current study suggest that ZnO NPs may increase M2 polarisation of macrophages. In the presence of ZnO NPs, expression levels of ARG-1 and IL-10 were increased but not those of inducible nitric oxide synthase, an enzyme that produces nitric oxide from L-arginine in M1 macrophages (Fig. S5). However, the exact role of ZnO NPs in macrophage polarisation warrants further investigation.

4. Conclusion

PEEK and PE polymer wear particles induced inflammation and osteolysis by activating the MEK–ERK pathway and COX-2 production. Nanoscale ZnO NPs (≤ 50 nm) at low concentration (5 μ g/mL) did not induce cytotoxicity and exerted anti-inflammatory effects *in vitro*. ZnO NPs attenuated PEEK or PE particle-induced inflammation and inflammatory osteolysis *in vivo* by reducing MEK and ERK phosphorylation and decreasing COX-2 expression. Topical use of ZnO NPs and polymer/ZnO NP blended composites may provide promising, effective approaches for inhibiting polymer wear particle-induced inflammatory osteolysis.

Declaration of competing interest

There are no conflicts to declare.

Acknowledgements

This study was supported by the National Key R&D Program of China [grant number 2016YFC1101802]; National Natural Science Foundation of China [grant number 81501855]; and Shanghai Sailing Program [grant number 15YF1407000].

Appendix A. Supplementary data

Supplementary data to this article can be found online at <https://doi.org/10.1016/j.jot.2022.04.001>.

References

- [1] Rankin KE, Dickinson AS, Briscoe A, Browne M. Does a PEEK femoral TKA implant preserve intact femoral surface strains compared with CoCr? A preliminary laboratory study. *Clin Orthop Relat Res* 2016;474(11):2405–13.
- [2] Du Z, Zhu Z, Yue B, Li Z, Wang Y. Feasibility and safety of a cemented PEEK-on-PE knee replacement in a goat model: a preliminary study. *Artif Organs* 2018;42(8):E204–e214.
- [3] Cowie RM, Briscoe A, Fisher J, Jennings LM. PEEK-OPTIMA™ as an alternative to cobalt chrome in the femoral component of total knee replacement: a preliminary study. *Proc IME H J Eng Med* 2016;230(11):1008–15.
- [4] Mbalaviele G, Novack DV, Schett G, Teitelbaum SL. Inflammatory osteolysis: a conspiracy against bone. *J Clin Invest* 2017;127(6):2030–9.
- [5] Naudie DD, Rorabeck CH. Sources of osteolysis around total knee arthroplasty: wear of the bearing surface. *Instr Course Lect* 2004;53:251–9.
- [6] Gallo J, Goodman SB, Konttinen YT, Wimmer MA, Holinka M. Osteolysis around total knee arthroplasty: a review of pathogenetic mechanisms. *Acta Biomater* 2013;9(9):8046–58.
- [7] Almasi D, Iqbal N, Sadeghi M, Sudin I, Abdul Kadir MR, Kamarul T. Preparation methods for improving PEEK's bioactivity for orthopedic and dental application: a review. *Int J Biomater* 2016;2016:8202653.
- [8] Lancaster JG, Dowson D, Isaac GH, Fisher J. The wear of ultra-high molecular weight polyethylene sliding on metallic and ceramic counterfaces representative of current femoral surfaces in joint replacement. *Proc IME H J Eng Med* 1997;211(1):17–24.
- [9] Meng X, Du Z, Wang Y. Feasibility of magnetic resonance imaging monitoring of postoperative total knee arthroplasty without metal artifacts: a preliminary study of a novel implant model. *BioMed Res Int* 2018;2018:8194670.
- [10] Meng X, Du Z, Wang Y. Characteristics of wear particles and wear behavior of retrieved PEEK-on-HXLPE total knee implants: a preliminary study. *RSC Adv* 2018;8(53):30330–9.
- [11] Heary RF, Parvathreddy N, Sampath S, Agarwal N. Elastic modulus in the selection of interbody implants. *J Spine Surg (Hong Kong)* 2017;3(2):163–7.
- [12] Du Z, Wang S, Yue B, Wang Y, Wang Y. Effects of wear particles of polyether-etherketone and cobalt-chromium-molybdenum on CD4- and CD8-T-cell responses. *Oncotarget* 2018;9(13):11197–208.

- [13] Du Z, Wang S, Wang Y. Preferential CD8 rather than CD4 T-cell response to wear particles of polyether-ether-ketone and highly cross-linked polyethylene. *RSC Adv* 2018;8(4):1866–74.
- [14] Fritz EA, Glant TT, Vermes C, Jacobs JJ, Roebuck KA. Chemokine gene activation in human bone marrow-derived osteoblasts following exposure to particulate wear debris. *J Biomed Mater Res* 2006;77(1):192–201.
- [15] Zhang L, Haddouti E-M, Welle K, Burger C, Wirtz DC, Schildberg FA, et al. The effects of biomaterial implant wear debris on osteoblasts. *Front Cell Dev Biol* 2020; 8:352.
- [16] Wojdasiewicz P, Poniatowski Ł A, Szukiewicz D. The role of inflammatory and anti-inflammatory cytokines in the pathogenesis of osteoarthritis. *Mediat Inflamm* 2014; 2014:561459.
- [17] Wang ML, Sharkey PF, Tuan RS. Particle bioreactivity and wear-mediated osteolysis. *J Arthroplasty* 2004;19(8):1028–38.
- [18] Liu W, Li J, Cheng M, Wang Q, Yeung KWK, Chu PK, et al. Zinc-modified sulfonated polyetheretherketone surface with immunomodulatory function for guiding cell fate and bone regeneration. *Adv Sci* 2018;5(10):1800749.
- [19] Shiel AI, Ayre WN, Blom AW, Hallam KR, Heard PJ, Payton O, et al. Development of a facile fluorophosphonate-functionalised titanium surface for potential orthopaedic applications. *J Orthop Translat* 2020;23:140–51.
- [20] Vilches F, Sanes J, Bermúdez M-D. Influence of ZnO nanoparticle filler on the properties and wear resistance of polycarbonate. *Wear* 2007;262:1504–10.
- [21] Liu J, Kang Y, Yin S, Chen A, Wu J, Liang H, et al. Key role of microtubule and its acetylation in a zinc oxide nanoparticle-mediated lysosome-autophagy system. *Small* 2019;15(25):e1901073.
- [22] Mirza EH, Pan-Pan C, Wan Ibrahim WM, Djordjevic I, Pinguan-Murphy B. Chondroprotective effect of zinc oxide nanoparticles in conjunction with hypoxia on bovine cartilage-matrix synthesis. *J Biomed Mater Res* 2015;103(11):3554–63.
- [23] Nagajyothi PC, Cha SJ, Yang LJ, Sreekanth TV, Kim KJ, Shin HM. Antioxidant and anti-inflammatory activities of zinc oxide nanoparticles synthesized using *Polygala tenuifolia* root extract. *J Photochem Photobiol B Biol* 2015;146:10–7.
- [24] Martínez-Carmona M, Gun'ko Y, Vallet-Regí M. ZnO nanostructures for drug delivery and theranostic applications. *Nanomaterials* 2018;8(4):268.
- [25] Yang C, Li J, Zhu K, Yuan X, Cheng T, Qian Y, et al. Puerarin exerts protective effects on wear particle-induced inflammatory osteolysis. *Front Pharmacol* 2019;10: 1113.
- [26] Meng X, Zhang J, Chen J, Nie B, Yue B, Zhang W, et al. KR-12 coating of polyetheretherketone (PEEK) surface via polydopamine improves osteointegration and antibacterial activity in vivo. *J Mater Chem B* 2020;8(44):10190–204.
- [27] Gaspar EB, Sakai YI, Gaspari ED. A mouse air pouch model for evaluating the immune response to *Taenia crassiceps* infection. *Exp Parasitol* 2014;137:66–73.
- [28] Longhofer LK, Chong A, Strong NM, Wooley PH, Yang S-Y. Specific material effects of wear-particle-induced inflammation and osteolysis at the bone-implant interface: a rat model. *J Orthopaed Transl* 2017;8:5–11.
- [29] Meng J, Zhou C, Hu B, Luo M, Yang Y, Wang Y, et al. Stevioside prevents wear particle-induced osteolysis by inhibiting osteoclastogenesis and inflammatory response via the suppression of TAK1 activation. *Front Pharmacol* 2018;9:1053.
- [30] Sahu D, Kannan GM, Vijayaraghavan R. Size-dependent effect of zinc oxide on toxicity and inflammatory potential of human monocytes. *J Toxicol Environ Health Part A* 2014;77(4):177–91.
- [31] Woodell-May JE, Sommerfeld SD. Role of inflammation and the immune system in the progression of osteoarthritis. *J Orthop Res* 2020;38(2):253–7. official publication of the Orthopaedic Research Society.
- [32] Liu J, Feng X, Wei L, Chen L, Song B, Shao L. The toxicology of ion-shedding zinc oxide nanoparticles. *Crit Rev Toxicol* 2016;46(4):348–84.
- [33] Hallab NJ, McAllister K, Brady M, Jarman-Smith M. Macrophage reactivity to different polymers demonstrates particle size- and material-specific reactivity: PEEK-OPTIMA® particles versus UHMWPE particles in the submicron, micron, and 10 micron size ranges. *J Biomed Mater Res B Appl Biomater* 2012;100(2): 480–92.
- [34] Liu A, Richards L, Bladen CL, Ingham E, Fisher J, Tipper JL. The biological response to nanometre-sized polymer particles. *Acta Biomater* 2015;23:38–51.
- [35] Yang S, Zhang K, Li F, Jiang J, Jia T, Yang SY. Biological responses of preosteoblasts to particulate and ion forms of Co-Cr alloy. *J Biomed Mater Res* 2015;103(11): 3564–71.
- [36] Limmer A, Wirtz DC. Osteoimmunology: influence of the immune system on bone regeneration and consumption. *Z. Orthop. Unfallchirurgie* 2017;155(3):273–80.
- [37] Hukkanen M, Corbett SA, Batten J, Kontinen YT, McCarthy ID, MacLouf J, et al. Aseptic loosening of total hip replacement. Macrophage expression of inducible nitric oxide synthase and cyclo-oxygenase-2, together with peroxynitrite formation, as a possible mechanism for early prosthesis failure. *J Bone Jt Surg Br Vol* 1997; 79(3):467–74.
- [38] Zhang X, Morham SG, Langenbach R, Young DA, Xing L, Boyce BF, et al. Evidence for a direct role of cyclo-oxygenase 2 in implant wear debris-induced osteolysis. *J Bone Miner Res : Off J Am Soc Bone Miner Res* 2001;16(4):660–70.
- [39] Li H, Zhang S, Huo S, Tang H, Nie B, Qu X, et al. Effects of staphylococcal infection and aseptic inflammation on bone mass and biomechanical properties in a rabbit model. *J Orthop Translat* 2020;21:66–72.
- [40] Nam JS, Sharma AR, Jagga S, Lee DH, Sharma G, Nguyen LT, et al. Suppression of osteogenic activity by regulation of WNT and BMP signaling during titanium particle induced osteolysis. *J Biomed Mater Res* 2017;105(3):912–26.
- [41] Tsutsumi R, Xie C, Wei X, Zhang M, Zhang X, Flick LM, et al. PGE2 signaling through the EP4 receptor on fibroblasts upregulates RANKL and stimulates osteolysis. *J Bone Miner Res : Off J Am Soc Bone Miner Res* 2009;24(10):1753–62.
- [42] Ren K, Dusat A, Zhang Y, Wang D. Therapeutic intervention for wear debris-induced aseptic implant loosening. *Acta Pharm Sin B* 2013;3(2):76–85.
- [43] Eliopoulos AG, Dumitru CD, Wang CC, Cho J, Tschlis PN. Induction of COX-2 by LPS in macrophages is regulated by Tpl2-dependent CREB activation signals. *EMBO J* 2002;21(18):4831–40.
- [44] Li Y, Pan Q, Xu J, He X, Li HA, Oldridge DA, et al. Overview of methods for enhancing bone regeneration in distraction osteogenesis: potential roles of biomaterials. *J Orthop Translat* 2021;27:110–8.
- [45] Maret W. Zinc in cellular regulation: the nature and significance of "zinc signals. *Int J Mol Sci* 2017;18(11):2285.
- [46] Sreejit G, Fleetwood AJ, Murphy AJ, Nagareddy PR. Origins and diversity of macrophages in health and disease. *Clin Transl Immunol* 2020;9(12):e1222.
- [47] Dierichs L, Kloubert V, Rink L. Cellular zinc homeostasis modulates polarization of THP-1-derived macrophages. *Eur J Nutr* 2018;57(6):2161–9.